NeuroImage: Clinical 13 (2017) 271–279

Contents lists available at ScienceDirect

NeuroImage: Clinical

journal homepage: www.elsevier.com/locate/ynicl

Cholinergic depletion and basal forebrain volume in primary progressive aphasia

Jolien Schaeverbeke[a,b,c], Charlotte Evenepoel[a,b,c], Rose Bruffaerts[a,d], Koen Van Laere[c,e], Guy Bormans[e,g], Eva Dries[d], Thomas Tousseyn[h], Natalie Nelissen[a,j], Ronald Peeters[i], Mathieu Vandenbulcke[b,f], Patrick Dupont[a,b,c], Rik Vandenberghe[a,b,c,d,*]

[a] Laboratory for Cognitive Neurology, Department of Neurosciences, KU Leuven, Herestraat 49, Box 1027, Leuven 3000, Belgium
[b] Alzheimer Research Centre, KU Leuven, Herestraat 49, Leuven 3000, Belgium
[c] Leuven Institute of Neuroscience and Disease, Herestraat 49, Leuven 3000, Belgium
[d] Neurology Department, University Hospitals Leuven, Herestraat 49, Leuven 3000, Belgium
[e] Nuclear Medicine and Molecular Imaging, KU Leuven and University Hospitals Leuven, Herestraat 49, Leuven 3000, Belgium
[f] Old Age Psychiatry Department, University Hospitals Leuven, Herestraat 49, Leuven 3000, Belgium
[g] Laboratory of Radiopharmaceutical Chemistry, KU Leuven, Herestraat 49, Leuven 3000, Belgium
[h] Pathology Department, University Hospitals Leuven, Herestraat 49, Leuven 3000, Belgium
[i] Radiology Department, University Hospitals Leuven, Herestraat 49, Leuven 3000, Belgium
[j] Experimental Psychology Department, Oxford University, 9 South Parks Road, Oxford OX1 3UD, United Kingdom

ARTICLE INFO

Article history:
Received 13 July 2016
Received in revised form 21 October 2016
Accepted 26 November 2016
Available online 2 December 2016

Keywords:
Kinetic modeling
Basal forebrain
Acetylcholinesterase
N-[^{11}C]-Methylpiperidin-4-yl propionate
PET
Primary progressive aphasia

ABSTRACT

Primary progressive aphasia (PPA) is a heterogeneous syndrome with various neuropathological causes for which no medical treatment with proven efficacy exists. Basal forebrain (BF) volume loss has been reported in PPA but its relation to cholinergic depletion is still unclear. The primary objective of this study was to investigate whether cholinergic alterations occur in PPA variants and how this relates to BF volume loss. An academic memory clinic based consecutive series of 11 PPA patients (five with the semantic variant (SV), four with the logopenic variant (LV) and two with the nonfluent variant (NFV)) participated in this cross-sectional *in vivo* PET imaging study together with 10 healthy control subjects. Acetylcholinesterase (AChE) activity was quantitatively measured in the neo- and allocortex using N-[^{11}C]-Methylpiperidin-4-yl propionate (PMP)-PET with arterial sampling and metabolite correction. Whole brain and BF volumes were quantified using voxel-based morphometry on high-resolution magnetic resonance imaging (MRI) scans.
In the PPA group, only LV cases showed decreases in AChE activity levels compared to controls. Surprisingly, a substantial number of SV cases showed significant AChE activity increases compared to controls. BF volume did not correlate with AChE activity levels in PPA. To conclude, in our sample of PPA patients, LV but not SV was associated with cholinergic depletion. BF atrophy in PPA does not imply cholinergic depletion.

© 2016 The Authors. Published by Elsevier Inc. This is an open access article under the CC BY-NC-ND license (http://creativecommons.org/licenses/by-nc-nd/4.0/).

1. Introduction

Primary progressive aphasia (PPA) is characterized by an isolated language impairment and is divided clinically into the subtypes of logopenic (LV), nonfluent (NFV) and semantic variant (SV) aphasia (Gorno-Tempini et al., 2011; Vandenberghe, 2016). Of the LV cases, 50–60% have underlying Alzheimer's disease (AD) pathology. In 50–70% of NFV cases the underlying cause is frontotemporal lobar degeneration (FTLD)-tauopathy (*i.e.* corticobasal degeneration (CBD), progressive supranuclear palsy (PSP) or Pick's disease pathology) and 69–83% of SV cases have FTLD-Transactive response DNA binding Protein 43 kDa (TDP-43) type C pathology (Grossman, 2010; Vandenberghe, 2016). Cholinergic depletion has been documented in typical AD (Bohnen et al., 2005, 2003; Kuhl et al., 1999), but it is currently unknown whether a cholinergic deficit also occurs in atypical AD presenting as PPA or in PPA due to a tauopathy or TPD-43 proteinopathy.

According to MRI volumetric studies, the basal forebrain (BF) is atrophic in PPA SV and NFV (Teipel et al., 2016, 2014), and mainly so the posterior part of the nucleus basalis (Ch4) and nucleus subputaminalis (NSP). The BF is the primary source of cholinergic transmission to the neo- and allocortex (Zaborszky et al., 2015), hence the hypothesis that a cholinergic deficit may also exist in non-AD cases of PPA.

* Corresponding author at: Neurology Department, University Hospitals Leuven, Herestraat 49, Box 7003, Leuven 3000, Belgium.
E-mail address: rik.vandenberghe@uzleuven.be (R. Vandenberghe).

http://dx.doi.org/10.1016/j.nicl.2016.11.027
2213-1582/© 2016 The Authors. Published by Elsevier Inc. This is an open access article under the CC BY-NC-ND license (http://creativecommons.org/licenses/by-nc-nd/4.0/).

Post mortem morphometric studies of the BF have mainly focused on AD or on FTLD-tau. In AD, severe degeneration of the BF, mainly the posterior part of Ch4, has been reported (Baker-Nigh et al., 2015; Grothe et al., 2014; Kerbler et al., 2015; Teipel et al., 2005). In FTLD-tau, Ch4 degeneration has been shown in PSP (Kasashima and Oda, 2003; Tagliavini et al., 1984), whereas both degeneration (Kasashima and Oda, 2003) and preservation (Dickson, 1999) of Ch4 have been reported in CBD.

Cholinergic denervation resulting from BF volume loss may be reflected in altered AChE activity levels. AChE activity levels can be mapped *in vivo* using N-[^{11}C]-Methyl-4-piperidyl acetate ([^{11}C]MP4A)- or N-[^{11}C]-Methylpiperidin-4-yl propionate ([^{11}C]PMP)-PET (Irie et al., 1996). The rate-dependent enzyme for acetylcholine (ACh) degradation *i.e.* acetylcholinesterase (AChE) is present at pre- and postsynaptic neurons (Wevers, 2011) and in a soluble form at the synaptic cleft (Schegg et al., 1992).

Studies using [^{11}C]MP4A and [^{11}C]PMP-PET have shown thalamic cholinergic depletion in PSP (Hirano et al., 2010; Shinotoh et al., 1999) and cortical cholinergic depletion in CBD (Shinotoh, 2007) and typical AD. Reduced AChE levels, as measured with [^{11}C]PMP-PET, have also been found in the neocortex and thalamus in two patients with FTDP-17 mutations (Hirano et al., 2006).

To date, no PET study investigated the cholinergic system in PPA exclusively.

The primary objective of this study was to investigate whether cholinergic alterations occur in PPA and how this depends on the variant. Cholinergic activity is crucial for several cognitive processes (Wevers, 2011) and plays a hypothetical role in language (Boban et al., 2006; Simić et al., 1999). As a consequence, a cholinergic deficit in PPA may have implications for therapeutic interventions.

2. Materials and methods

2.1. Subjects

Patients were recruited between 2004–2006 and between 2009 and 2015 at the memory clinic University Hospitals Leuven. Each PPA case was diagnosed according to Gorno-Tempini et al., 2011 recommendations (Gorno-Tempini et al., 2011). Healthy control subjects were recruited through advertisement in local newspapers or internet. Eleven patients with PPA (five SV, four LV and two NFV) (Table 1) participated as well as 10 control subjects. Three patients received a neuropathological examination (interval from [^{11}C]PMP-PET till death: 6.00 ± 3.61 years). LV case 8 received a diagnosis of pathologically definite AD 3 years *post* [^{11}C]PMP-PET, NFV case 1 a diagnosis of pathologically definite CBD 5 years *post* [^{11}C]PMP-PET and SV case 9 a diagnosis of pathologically definite FTLD with TDP-43 inclusions subtype I pathology 10 years *post* [^{11}C]PMP-PET. There was no significant history of stroke, psychiatric illness or vascular disease in study participants. Patients were naive for cholinesterase inhibitors and none of the study participants took anticholinergic medication. All subjects received a [^{11}C]PMP-PET scan along with a volumetric MRI scan. For MRI volumetric comparisons, we included an additional set of 24 healthy controls (67.3 ± 8.83 years), scanned on the same scanner, as well as 17 additional PPA patients (4 LV, 6 NFV and 7 SV) (Table 1) (Grube et al., 2016) and 77 additional controls (64.6 ± 5.86 years) who were scanned on a different scanner (see MRI acquisition and analysis).

The study was approved by the Ethics Committee, University Hospitals Leuven. All participants provided written informed consent in accordance with the Declaration of Helsinki.

Table 1
Demographics and neuropsychological characteristics.

Case	PPA	*Post mortem*	Age (y)	Symptom duration (y)	Gender	CDR	BNT	PALPA	AAT-compr	BORB-hard	BORB-easy	CPM
5[b]	LV	/	59	2.5	m	2	/	15[a]	83[a]	21[a]	27[a]	20[a]
6[b]	LV	/	77	2	m	1	39[a]	25	102[a]	22[a]	30	29
7[b]	LV	/	66	3	m	1	35[a]	27	94[a]	23a	32	23[a]
8[b]	LV	AD	72	2.5	f	1	24[a]	26	83[a]	25	29	17
13	LV	/	57	0.5	f	0.5	56	28	120	25	29	35
17	LV	/	64	3	m	0.5	41[a]	23[a]	114	25	31	33
23	LV	/	71	1	m	0	53	28	118	26	31	33
18	LV	/	62	1.5	f	1	53	27	106	24	31	31
1[b]	NFV	CBD	77	3	m	1	43[a]	25	105	21[a]	30	24[a]
11[b]	NFV	/	71	2.5	m	1	45[a]	29	112	27	30	21[a]
15	NFV	/	52	2	f	2	58	28	120	26	31	31
20	NFV	/	79	5	f	1	48	22[a]	105	25	30	24[a]
22	NFV	/	71	1.5	m	0.5	55	28	102[a]	26	31	24[a]
26	NFV	/	78	2.5	m	1	48	23[a]	77[a]	26	29	30
27	NFV	/	72	2.5	f	1	30[a]	19[a]	85[a]	21[a]	18[a]	12[a]
28	NFV	/	63	5	f	0	41[a]	24[a]	104[a]	22[a]	28	32
2[b]	SV	/	59	4	m	1	36[a]	22[a]	78[a]	17[a]	23[a]	21[a]
3[b]	SV	/	63	3	f	1	14[a]	24[a]	95[a]	22[a]	25[a]	23[a]
4[b]	SV	/	71	6	m	1	13[a]	22[a]	95[a]	24	28	17[a]
9[b]	SV	TDP-43 I	52	1.5	f	1	/	17[a]	62[a]	21[a]	23[a]	36
10[b]	SV	/	57	2	m	1	14[a]	22[a]	87[a]	19[a]	26[a]	34
12	SV	/	76	6	m	1	34[a]	27	90[a]	20[a]	23[a]	29
14	SV	/	70	1.5	f	1	22[a]	17[a]	74[a]	20[a]	18[a]	24[a]
16	SV	/	61	3	m	2	7[a]	18[a]	73[a]	18[a]	20[a]	36
19	SV	/	64	3	m	1	20[a]	14[a]	74[a]	18[a]	26[a]	29
21	SV	/	48	6	f	1	12[a]	24[a]	82[a]	17[a]	26[a]	35
24	SV	/	58	2	f	1	35[a]	27	93[a]	27	31	36
25	SV	/	68	5	f	1	16[a]	23[a]	114	25	31	34
Groupdata	PPA	Mean (SD)	65.8(8.5)	2.96(1.5)	13f/15m	0.89	34.3(15.7)	23.4(4.2)	94.5(16.1)	22.6(3.1)	27.4(4.1)	27.6(6.7)
	Controls	Mean (SD)	65.4(6.7)	/	48f/63m	0	53.7 (4.7)	27.6(1.8)	114.8(4.8)	27.2(1.97)	29.8(1.5)	32.2(3.2)
		p	0.7	/	0.92	<0.001	<0.001	<0.001	<0.001	<0.001	0.01	0.005

Abbreviations: AAT = Aachen aphasia test, comprehension (/120), BORB-hard/-easy = Birmingham object recognition battery (/32), BNT = Boston Naming test (/60), CBD = corticobasal degeneration, CDR = Clinical dementia rating scale, CPM = colored progressive matrices (/36), PALPA = Psycholinguistic assessment of language in aphasia, subtest 49: associative-semantic task for words (/30). PPA variants: LV = logopenic variant, NFV = nonfluent variant, SV = semantic variant PPA patients.

[a] Scores which are significantly different compared to controls based on a modified *t*-test.

[b] Patients who received [^{11}C]PMP-PET.

All subjects underwent extensive neuropsychological testing. Global cognitive functioning was assessed by the clinical dementia rating scale (CDR). Language was assessed by means of the 60-item version of the Boston Naming test (BNT), the validated Dutch version of the Aachen Aphasia test (AAT) and the verbal semantic association test of the psycholinguistic assessment of language processing in aphasia (PALPA subtest 49). Visual recognition of objects was assessed by the object decision test of the Birmingham object recognition battery (BORB) hard and easy. Fluid intelligence and reasoning ability were quantified by the Raven's colored progressive matrices (CPM).

2.2. PET acquisition and analysis

[^{11}C]PMP was synthesized as described previously (Snyder et al., 1998). The injected activity was 261.3 ± 28.31 MBq in control subjects and 290.3 ± 62.6 MBq in PPA patients. Dynamic PET data were acquired in 3D mode during 60 min (rebinned in 4 × 15 s, 4 × 1 min, 2 × 2.5 min, 10 × 5 min) on a Siemens/ECAT EXACT HR + PET scanner (CTI PET System, Inc., Knoxville, TN 37932, USA). Data were reconstructed using 3D-filtered back-projection with a Hanning filter with cut-off frequency of 0.5 of the Nyquist frequency, corrected for random scatter, attenuation and decay and smoothed with a 6 mm isotropic full-width at half-maximum (FWHM) Gaussian 3D kernel.

For each subject 19 arterial samples were collected during the scan period to determine the individual plasma time-activity curve (TAC). Seven additional samples were used for metabolite correction. One LV PPA patient (case 6) (Table 1) and one control subject had to be excluded due to arterial sampling problems. One control subject was excluded based on excessive movement during PET scan acquisition. The remaining eight control subjects and 10 PPA patients were included in our PET-based analyses.

Blood samples were centrifuged, and the radioactive plasma was subsequently eluted on high-performance liquid chromatography and counted in a gamma counter. The intact fractions of tracer over time were fitted using a constrained Hill model as metabolite correction function and this function was used to correct the plasma input function.

PET images were processed using Statistical Parametric Mapping 8 (SPM8, Wellcome Trust Centre for Neuroimaging, London, UK). For each subject, subject-specific volumes of interest (VOI) were calculated by intersecting the subjects normalized gray matter (GM) map (thresholded at >0.25) with each automatic anatomic labeling (AAL) (Tzourio-Mazoyer et al., 2002) VOI. With the metabolite-corrected plasma TACs as input, regional brain TACs were fitted to the theoretical two-tissue three-rate constant compartment model including a cerebral blood volume fraction. This model characterizes rate constants for influx (K_1, min^{-1}) and efflux (k_2, min^{-1}) across the blood-brain barrier (first tissue compartment) and the rate of hydrolysis (k_3, min^{-1}) of [^{11}C]PMP (second tissue compartment) (Koeppe et al., 1999). The k_3 values were calculated for each subject-specific VOI (Fig. A.1). These k_3 values are a proxy for AChE activity levels in the brain (Koeppe et al., 1999). Left and right hemispheres were analyzed separately. To reduce spillover from high uptake regions to regions with low or moderate uptake, we additionally applied a mask in VOIs with low or moderate uptake. This mask contained all voxels with high uptake values across all control subjects and as a result, it excluded these voxels within VOIs with low or moderate uptake (spill-over correction). We then calculated a weighted mean k_3 value by taking into account the size of each subject-specific VOI of the left and right neocortex (including frontal, parietal, temporal and occipital neocortical VOIs) and left and right allocortex (including olfactory gyrus, amygdala, hippocampus and parahippocampal gyrus VOIs) to obtain weighted mean k_3 values in known projection regions of the BF (Mesulam, 2013).

2.3. MRI acquisition and analysis

The 11 PPA and 10 HC received a T_1-weighted structural MRI on a 1.5T Siemens Sonata system (Siemens Medical Solutions, Erlangen, Germany) and eight-channel head coil (coronal inversion recovery prepared 3D gradient-echo images; inversion time (TI) 800 milliseconds (ms), echo time (TE) = 3.93 ms, voxel size (1 × 1 × 1) mm^3).

Preprocessing of the T_1-weighted images was performed with Voxel-Based Morphometry 8 (VBM8) (Ashburner and Friston, 2000), implemented in Matlab R2012b as described previously (Gillebert et al., 2015). This procedure generated non-linear only modulated GM maps, corrected for total intracranial volumetric differences. These GM maps were used to obtain mean BF GM volumes by averaging the unsmoothed modulated warped GM voxel values within the BF mask (Kilimann et al., 2014). All BF volumes have been adjusted for overall brain size by using only the nonlinear component of the spatial normalization for modulation of GM voxel intensities.

In order to determine whether any AChE changes occurred specifically in regions that were typically affected in a particular subtype, an extended sample of PPA and controls were analyzed to determine the regions of subtype-specific atrophy with high sensitivity. In addition to the initial sample of 11 PPA and 10 control subjects, this extended sample contained 24 additional controls who had undergone a volumetric research MRI on the same scanner using the same sequence as mentioned above as well as 17 additional PPA (4 LV, 6 NFV and 7 SV) (Grube et al., 2016) and 77 additional controls who had undergone a T_1-weighted structural MRI on a 3T Philips Intera system and an eight-channel head coil (coronal inversion recovery prepared 3D gradient-echo images; TI 900 ms, TE = 4.6 ms, voxel size (0.98 × 0.98 × 1.2) mm^3).

To identify subtype-specific atrophy, we contrasted the group of 28 PPA cases to the 111 controls in a voxelwise ANCOVA in SPM8 with smoothed modulated GM volume maps as within-subject factor, group (4 levels: LV, SV, NFV, healthy controls) as between-subject factor and age, gender and scanner as nuisance variables. Results were considered significant at voxel-level uncorrected $p < 0.001$ combined with cluster-level family-wise error (FWE)-corrected $p < 0.05$ (Poline et al., 1997). For voxelwise statistical comparisons, GM maps were smoothed with an 8 mm isotropic FWHM Gaussian 3D kernel.

2.4. Statistics

Standard statistical analyses were performed in Statistics Software Package for the Social Sciences (version 23, IBM Statistics, Armonk, USA).

BF volumes and AChE activity levels were checked for outliers using the Grubbs' test: Z scores higher than three standard deviations were classified as outliers. The individuals' Neuropsychological test scores were compared to controls using a modified *t*-test (Crawford and Garthwaite, 2012) (Table 1). Differences in age between PPA patients and control subjects were assessed using Kruskal-Wallis and with Pearson chi^2 tests for gender.

2.4.1. Primary outcome analyses

Given the relatively limited sample size, the primary analysis was based on a multiple single case series methodology. Differences of AChE activity levels in global neo- and the global allocortical VOIs in the left and right hemisphere were assessed in each individual patient in comparison to the eight controls using a modified *t*-test (Crawford and Garthwaite, 2012).

As a second primary outcome analysis, a Spearman or Pearson correlational analysis was performed between AChE activity levels averaged over left and right allo- and neocortex, and BF volume, depending on normality of the data.

2.4.2. Secondary outcome analyses

Secondary outcome analyses aimed to evaluate effects at the overall group and at the subgroup level, to examine the relationship between the AChE activity levels and structural changes, and to test the replicability of the BF atrophy in PPA reported previously (Teipel et al., 2016, 2014).

1. Differences in AChE activity were assessed at the group level (PPA *versus* controls) using Kruskal-Wallis and with *post hoc* Mann-Witney *U* tests for differences between subgroups (uncorrected, two-tailed *p* values).
2. In order to evaluate the relationship between AChE activity levels and structural atrophy, AChE activity levels were calculated in each individual patient compared to controls in the regions that were characteristically atrophic for the subtype to which the case belonged (LV, NFV or SV) (VOI shown in Fig. 3). In order to determine whether AChE activity levels were specifically lower in the atrophic regions, AChE activity levels were also evaluated in cortical regions falling outside subtype-specific regions of atrophy. The latter region was determined by subtracting the region of characteristic atrophy from the subjects normalized GM map (thresholded at >0.25). For each individual patient, differences in AChE levels compared to controls were assessed using a modified *t*-test.
3. In order to evaluate whether BF volume decreases that have previously been reported (Teipel et al., 2016, 2014) could be replicated, a BF volume analysis was performed in the extended sample of 28 PPA and 111 control subjects. By means of an ANCOVA model, BF volumes were assessed at the group level in controls, LV, NFV and SV PPA with scanner type as nuisance variable, and *post hoc* Bonferroni correction for the number of comparisons at $\alpha = 0.05$.
4. Finally, we determined the effects of symptom duration, age, and gender on AChE activity levels by means of Spearman or Pearson correlational analyses or Mann Witney *U* tests (two-tailed).

3. Results

3.1. Primary outcome analyses

3.1.1. AChE activity levels in PPA patients

Two out of three LV patients showed significantly lower neocortical AChE activity levels than controls in the left (case 7: $t = -2.68$, $p = 0.016$ and case 8: $t = -4.12$, $p = 0.002$) (Fig. 1A) and in the right hemisphere (case 7: $t = -3.17$, $p = 0.008$ and case 8: $t = -5.59$, $p < 0.001$) (Fig. 1B). No differences were found in NFV or SV cases compared to controls (all $p > 0.13$) (Fig. 1A, B).

In two out of three LV patients, left allocortical AChE activity levels were significantly lower than in controls (case 7: $t = -1.93$, $p = 0.047$ and case 8: $t = -2.70$, $p = 0.015$) (Fig. 1C). In one of these cases, right-hemispheric allocortical AChE activity levels were also lower compared to controls (case 8: $t = -4.20$, $p = 0.002$) (Fig. 1D).

Four out of five SV patients showed significantly elevated right allocortical AChE activity levels (case 3: $t = 3.39$, $p = 0.006$; case 4: $t = 4.57$, $p = 0.001$; case 9: $t = 2.26$, $p = 0.029$; case 10: $t = 3.28$,

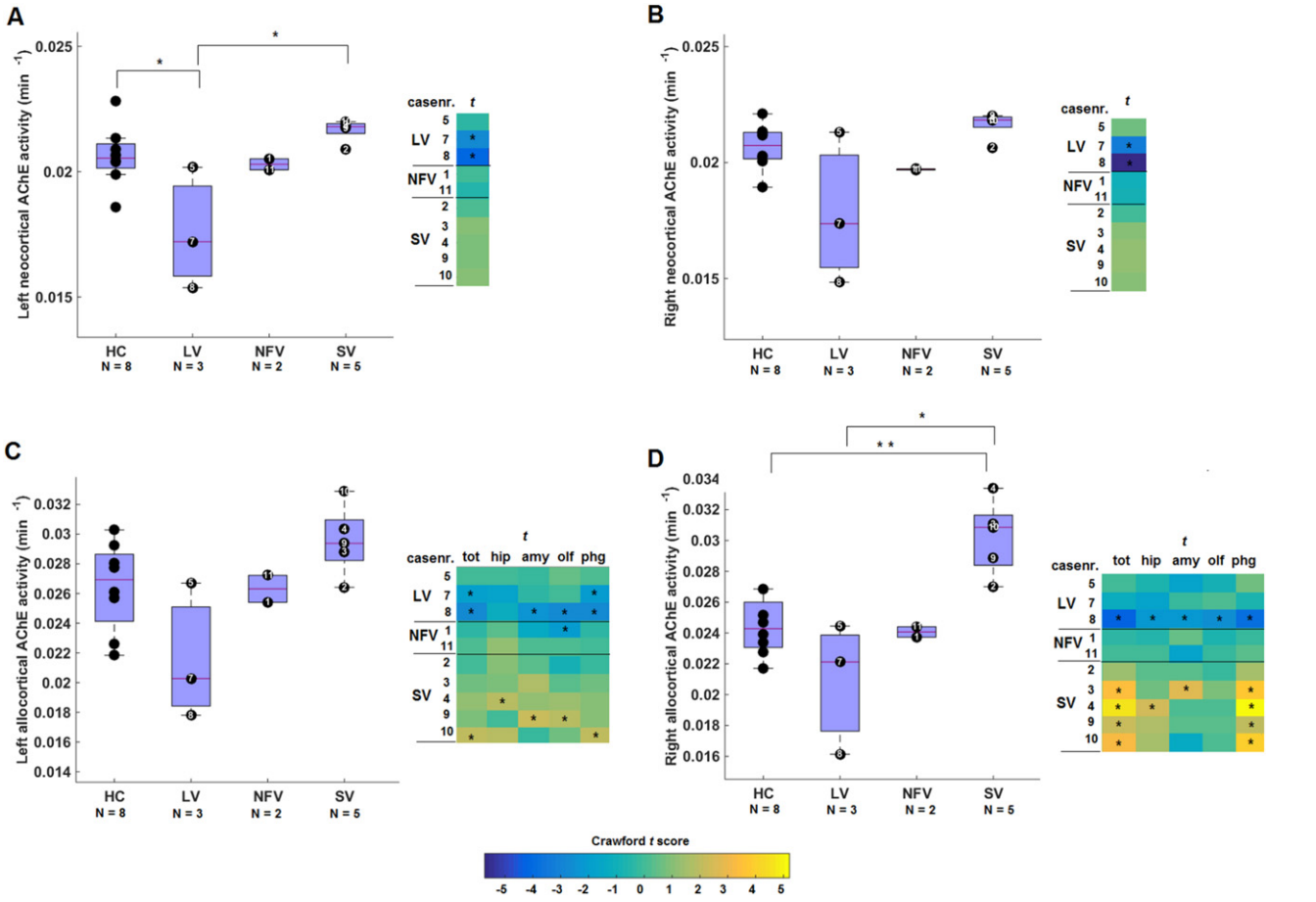

Fig. 1. Acetylcholinesterase activity levels. AChE activity levels are plotted for (A) left and (B) right neocortex and for (C) left and (D) right allocortex. Boxplot: minimum, first quartile, median (red line), third quartile, and maximum. Color bar: *t* scores for individual AChE activity levels based on a modified *t*-test with a threshold of $\alpha = 0.05$. Patients who significantly differed from controls based on the modified *t*-test are indicated with an asterisk on the color bar. For group based comparisons: $^{*}p < 0.05$, $^{**}p < 0.01$. Abbreviations: amy = amygdala, HC = healthy controls, hip = hippocampus, LV = logopenic variant, NFV = nonfluent variant, olf = olfactory gyrus, phg = parahippocampal gyrus, SV = semantic variant PPA patients, tot = total region. Case nr. = case numbers corresponding to Table 1.

$p = 0.007$) (Fig. 1D). In one of these cases, left allocortical AChE activity levels were significantly higher than in controls (case 10: $t = 2.0$, $p = 0.042$) (Fig. 1C). No significant differences compared to controls were found in NFV patients (all $p > 0.37$).

In order to gain further insight in the elevation of allocortical AChE activity levels in SV cases, we analyzed each of the four subVOIs of which the allocortical VOI was composed. The elevation of AChE activity was mainly seen in the subVOI corresponding to the right parahippocampal gyrus (case 3: $t = 3.72$, $p = 0.004$, case 4: $t = 5.22$, $p < 0.001$, case 9: $t = 2.11$, $p = 0.036$ and case 10: $t = 3.93$, $p = 0.003$) and least so in the subVOI corresponding to the olfactory gyrus (case 9: $t = 1.95$, $p = 0.046$) (Fig. 1C and D).

3.1.2. Correlation between BF volume and AChE activity levels

BF volume in PPA patients did not correlate with AChE activity levels in the left (Spearman $\rho(8) = 0.16$, $p = 0.65$) or right neocortex (Pearson $\rho(8) = -0.37$, $p = 0.29$) (Fig. 2A and B), nor in the left (Pearson $\rho(8) = -0.24$, $p = 0.51$) or right allocortex (Pearson $\rho(8) = 0.28$, $p = 0.43$) (Fig. 2C and D).

3.2. Secondary outcome analyses

3.2.1. Group-based comparisons of AChE activity levels in neo- and allocortex

Left neocortical AChE activity differed significantly between groups ($chi^2(3) = 9.5$, $p = 0.024$). Only LV patients showed significantly lower left neocortical AChE activity levels compared to controls ($U = 2$, $p = 0.041$) and compared to SV patients ($U = 0$, $p = 0.025$). No differences were found between other subgroups (all $p > 0.053$) (Fig. 2A, B).

Right allocortical AChE activity levels were significantly different between groups ($chi^2(3) = 11.3$, $p = 0.010$) (Fig. 2D). SV patients had significantly elevated right allocortical AChE activity levels compared to controls ($U = 0$, $p = 0.003$) and compared to LV ($U = 0$, $p = 0.025$). No significant differences were found between other subgroups (all $p > 0.053$).

3.2.2. Topography of AChE activity changes versus topography of cortical volume loss in PPA

3.2.2.1. Definition of PPA atrophic regions. In the extended sample of PPA patients and controls, LV patients showed atrophy restricted to the left posterior third of the left middle temporal gyrus, extending towards the temporoparietal junction as well as bilateral atrophy of the precuneus (Fig. 3A). NFV patients exhibited atrophy of the bilateral supplementary motor area and cingulum, together with left inferior and middle frontal lobe atrophy extending towards the left insula (Fig. 3B). SV patients showed severe atrophy of the bilateral anterior temporal lobe, including the anterior fusiform gyri, as well as atrophy of the amygdalae, hippocampi and insulae (Fig. 3C).

Overall, there was a predominant left lateralization of atrophy independently of PPA subtype.

3.2.2.2. AChE activity levels in the PPA atrophic and preserved neocortical regions. At the individual patient level, two out of three LV patients showed lower AChE activity levels compared to controls in brain regions typically atrophic in LV PPA (case 7: $t = -2.65$, $p = 0.016$ and case 8: $t = -6.20$, $p < 0.001$) (Fig. 4A). These two LV patients showed also lower AChE activity levels (case 7: $t = -3.04$, $p = 0.009$ and case 8: $t = -4.73$, $p = 0.001$) compared to controls outside the regions that were typically atrophic in LV PPA (Fig. 4B). This suggests that the reduction in AChE activity levels is not restricted to the regions of characteristic atrophy in LV but is more diffuse.

Compared to controls, two of the five SV patients showed elevated AChE activity levels in regions typically atrophic in SV PPA (case 9: $t = 2.09$, $p = 0.038$; case 10: $t = 1.88$, $p = 0.05$) (Fig. 4A). SV patients did not show abnormal AChE activity levels outside the SV atrophic

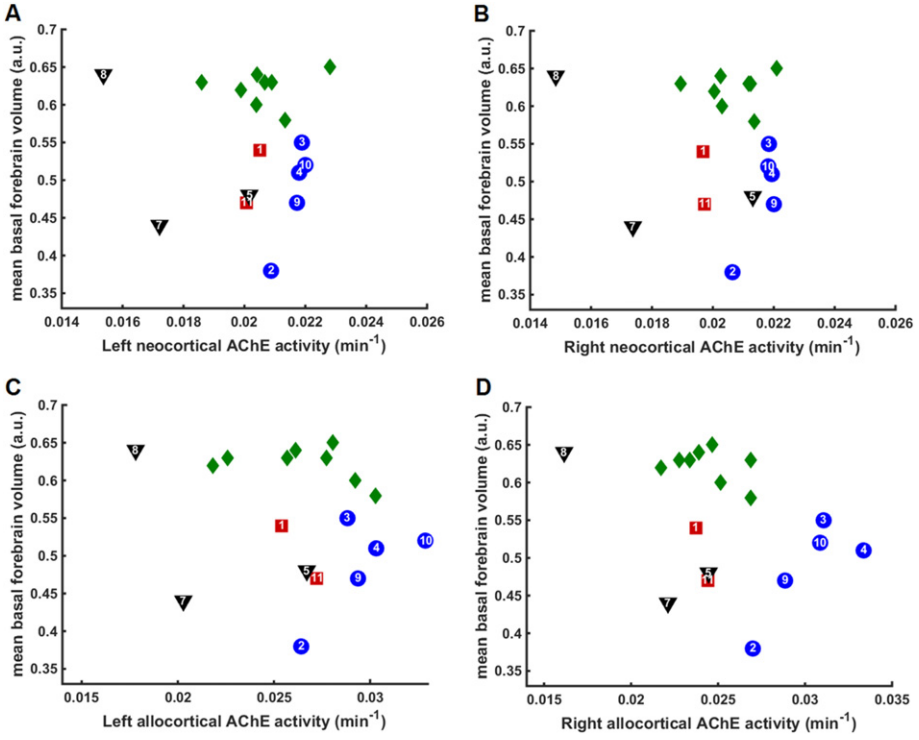

Fig. 2. Basal forebrain volume and AChE activity levels. AChE activity levels of (A) left and (B) right neocortex and (C) left and (D) right allocortex on the abscissa (min^{-1}) and mean basal forebrain volumes (arbitrary units) on the ordinate. Green diamonds: HC = healthy controls, black triangles: LV = logopenic variant, red squares: NFV = nonfluent variant, blue circles: SV = semantic variant PPA patients. Case numbers correspond to Table 1.

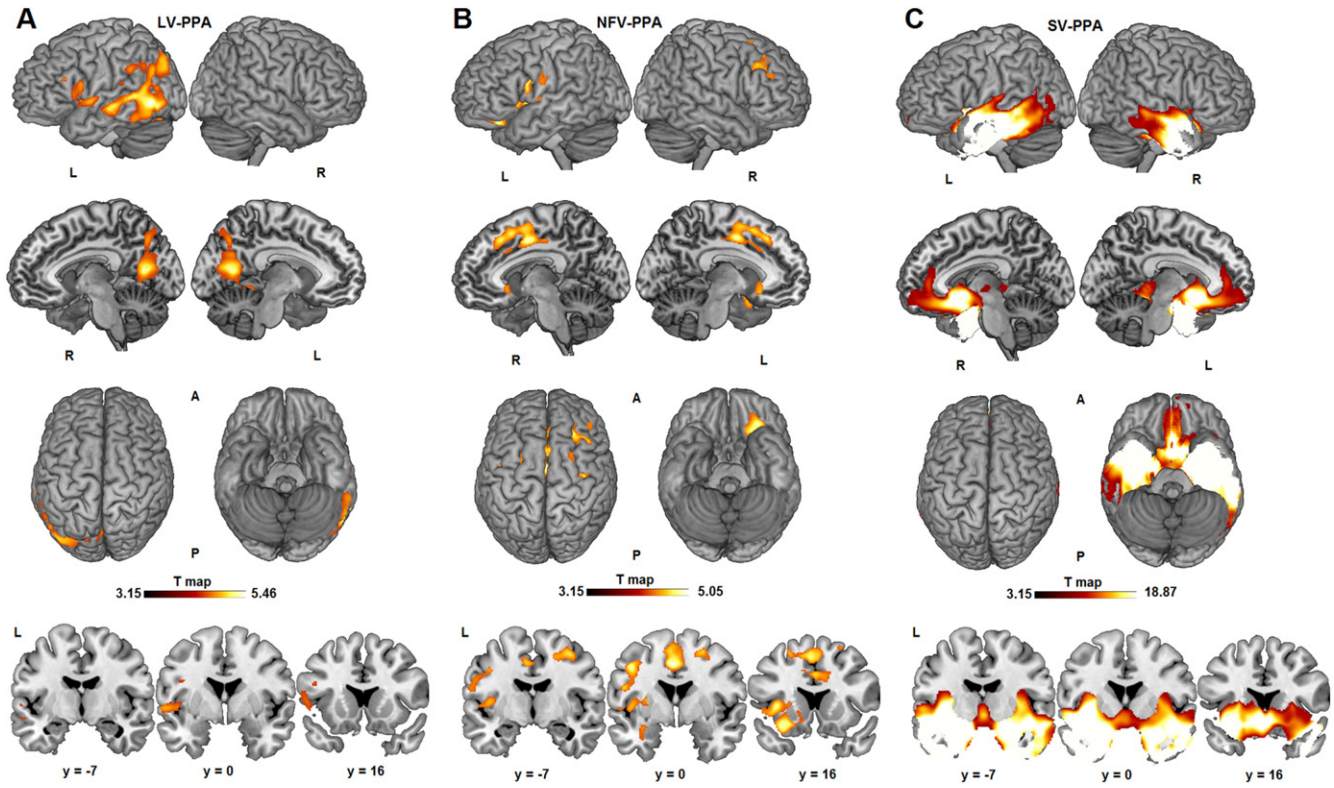

Fig. 3. Cortical atrophy patterns in PPA. *T*-maps, generated by contrasting each PPA subgroup (total N = 28) *versus* controls (N = 111) in SPM8, are projected onto a surface rendering of a template brain and on coronal slices with corresponding MNI coordinates. Threshold: voxel-level uncorrected $p < 0.001$ combined with cluster-level FWE-corrected $p < 0.05$. *T*-maps depict brain regions of reduced gray matter volume in (A) logopenic variant (LV), (B) nonfluent variant (NFV), and (C) semantic variant (SV) PPA patients.

regions (Fig. 4B). This may suggest that the increase in AChE activity levels in SV could potentially be most pronounced in those regions that are also most affected structurally. No significant differences were found for NFV patients compared to controls (all $p > 0.31$).

3.2.3. BF volumetry in the extended PPA sample

In the entire group of PPA patients, BF volume was reduced in three out of eight LV (case 5: $t = -1.75$, $p = 0.042$, case 7: $t = -2.41$, $p = 0.009$ and case 17: $t = -2.00$, $p = 0.023$), one out of eight NFV (case 11: $t = -1.91$, $p = 0.029$) and five out of 12 SV patients (case 2, $t = -3.42$, $p < 0.001$, case 9: $t = -1.91$, $p = 0.029$, case 14: $t = -2.45$, $p = 0.008$, case 19: $t = -2.56$, $p = 0.006$ and case 25: $t = -3.07$, $p = 0.001$) compared to controls (Fig. 5).

There was a significant overall effect of group on BF volume ($F(3134) = 11.8$, $p < 0.001$). *Post hoc* tests revealed that BF volume was most reduced in SV compared to controls ($-17.2 \pm 11\%$, $p < 0.001$). No significant differences were found in LV ($-7.3 \pm 13\%$, $p = 0.40$) or NFV ($-9.6 \pm 7.8\%$, $p = 0.07$) patients compared to controls. No significant differences of BF volume were found between PPA variants ($p > 0.1$) (Fig. 5).

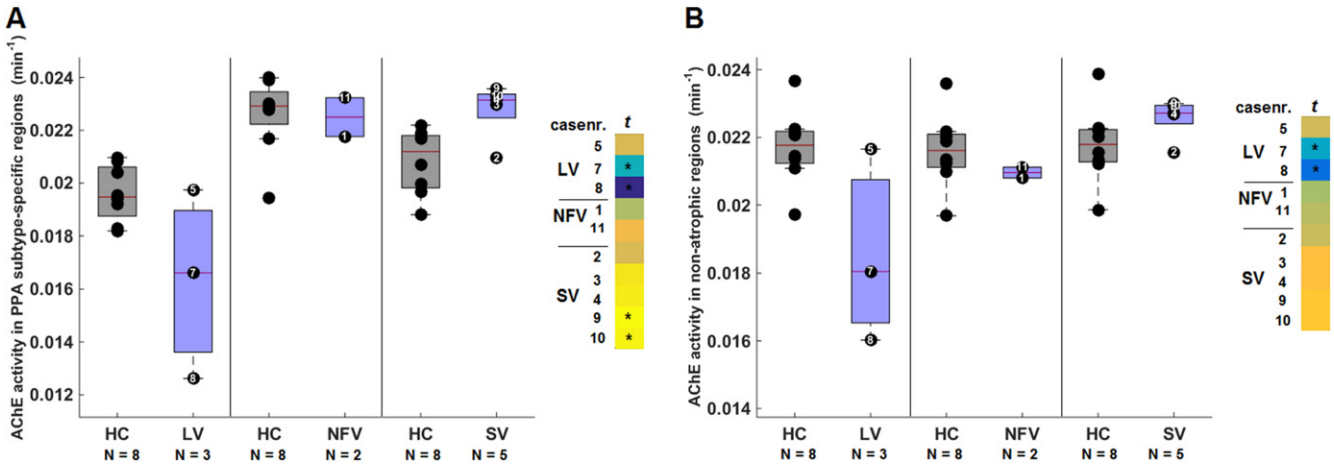

Fig. 4. AChE activity levels in subtype-specific PPA atrophic regions and in the associative-semantic network. AChE activity based on a modified *t*-test with a threshold of $\alpha = 0.05$ in (A) subtype-specific atrophy in PPA and (B) complementary non-atrophic brain regions. Note that the subtype-specific regions differed depending on the variant and that the values plotted for each subtype are obtained in the regions that are atrophic for that particular subtype. Accordingly, the corresponding values in the controls were obtained in that same subtype-specific region. Patients that significantly differed from controls are indicated with an asterisk on the color bar. Abbreviations: LV = logopenic variant, HC = healthy controls, NFV = nonfluent variant, SV = semantic variant. Case numbers correspond to Table 1.

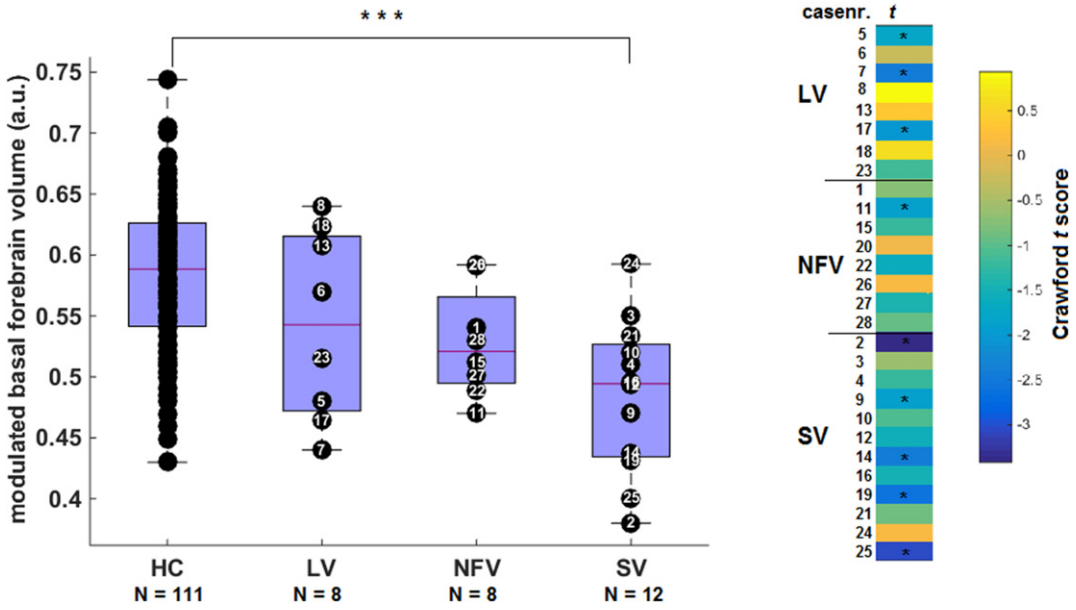

Fig. 5. Basal forebrain volume in PPA subtypes. Boxplot with BF volumes: minimum, first quartile, median (red line), third quartile, and maximum and color bar: *t* scores for individual BF volume based on a modified *t*-test with a threshold of $\alpha = 0.05$. Patients that significantly differed from controls are indicated with an asterisk on the color bar. For group based comparisons: ***$p < 0.001$. Abbreviations: HC = healthy controls, LV = logopenic variant, NFV = nonfluent variant, SV = semantic variant PPA patients. Case numbers correspond to Table 1.

3.2.4. Effects of age, gender and symptom duration on AChE activity

In the current PPA sample, there were no effects of symptom duration on AChE activity levels in the left or right neo- or allocortical region ($p > 0.30$) and no effects of age ($p > 0.098$) or gender ($p > 0.57$) on AChE activity levels.

4. Discussion

The current findings demonstrate that BF atrophy does not imply cholinergic depletion. The presence of BF atrophy in SV was replicated, however this was not associated with a cholinergic deficit. Instead AChE activity in SV was increased. Cholinergic depletion was only seen in LV cases, both within and outside the neocortical regions of characteristic atrophy.

4.1. Cholinergic alterations

The LV with pathologically definite AD (case 8) showed the strongest reductions in AChE activity levels. LV PPA can occur as an atypical variant of AD and 50–60% of cases show AD pathology (Matías-Guiu et al., 2015). Loss of the cholinergic systems integrity is among the earliest events in the pathogenesis of typical AD: several studies have shown reduced AChE activity in typical AD patients using [^{11}C]PMP-PET (Bohnen et al., 2005, 2003; Kuhl et al., 1999). The current study shows that this finding can be extended to a subset of LV PPA cases.

The reduction in AChE activity did not appear to be limited to regions typically affected by volume loss in LV PPA. AChE activity reductions were seen also outside regions of typical atrophy. If AChE activity reductions in LV are a consequence of neuronal loss in diffusely projecting subcortical nuclei such as Ch4, one would expect that the PET measure would not strictly overlap with the measure of regional volume loss.

Unexpectedly, despite the BF volume loss, SV PPA was associated with an increase in AChE activity levels. This increase was most pronounced in regions of maximal volume loss, both in the neocortical and in the allocortical regions such as the parahippocampal gyrus. The colocalisation between AChE activity increases and structural volume loss could possibly suggest that AChE activity increases are a compensatory mechanism and a reaction to neuronal loss in SV PPA. This increase was only observed in SV cases and the vast majority of SV PPA is caused by a TDP-43 proteinopathy (Grossman, 2010; Josephs et al., 2009). In the current study, SV case 9 received a diagnosis of pathologically definite FTLD with TDP-43 inclusions subtype I. A previous expression study in transgenic mice (Tg-VLW) expressing human tau mutations, suggested that tauopathy may be associated with AChE activity increases (Silveyra et al., 2012). This is the first study which showed AChE increases in a case with proven TDP-43 proteinopathy. It may be worth investigating how specific types of proteinopathy differentially affect neurotransmitter systems and the regional specificity of such effects.

Neuropathological examinations of other cholinergic biomarkers in semantic dementia showed that there is an increase in the proportion of cholinergic M2 muscarinic receptors compared to controls, with a decrease in the proportion of cholinergic M1 muscarinic receptors (Odawara et al., 2003). The increase in M2 receptors found by Odawara as well as the increase in AChE activity levels in the current study are possibly suggesting a compensatory reaction to the neurodegenerative neuronal loss.

Elevated AChE activity levels as measured with PET have previously been reported in FTD, although non-significantly and restricted to the thalamus (Hirano et al., 2010). However, most studies on FTD failed to show any abnormalities in AChE, be it *post mortem* (Procter et al., 1999) or at the level of cerebrospinal fluid (CSF) (Wallin et al., 2003).

4.2. BF atrophy and relation to cholinergic alterations

The BF receives afferents from the amygdala and hippocampus (Aggleton et al., 1987). On their turn, cholinergic pathways arising from the BF project among others to the temporal lobe and the parahippocampal gyrus (Selden et al., 1998). These regions are typically affected in SV PPA in cross-sectional (Mummery et al., 2000; Rosen et al., 2002; Whitwell et al., 2005) and longitudinal studies of the disease (Brambati et al., 2007).

BF volume loss in SV however was not associated with cholinergic depletion. The neuronal, glial and interstitial compartments that contribute to MRI measures of BF are far broader than the cholinergic neuronal cell population. For instance, cholinergic neurons are typically found intermingled with inhibitory interneurons, the second most important BF cell types (Mesulam, 2013).

Our data caution against inferences based upon MRI BF volume measures with regards to cholinergic status in PPA.

4.3. A cholinergic therapy for PPA?

There are currently no medications approved by the US Food and Drug Administration (FDA) to treat PPA. Language regions contain a relatively high density of AChE-containing neurons (Hutsler and Gazzaniga, 1991), which may suggest a rational basis for cholinergic treatment in PPA. Cholinergic therapy improves language in various disorders affecting the language network (Berthier et al., 2006; Ferris and Farlow, 2013; Tanaka et al., 1997; Yoon et al., 2015), although regulatory approval is restricted to clinically probable AD.

To date, only one study with an open-label period of 18 weeks and a randomized, placebo- controlled phase for eight weeks with galantamine included PPA patients (Kertesz et al., 2008). The overall language performance showed a trend towards stabilization over a total duration of eight weeks. A randomized, placebo- controlled study with memantine showed general good tolerance, however there were more frequent cognitive adverse events (Boxer et al., 2013). A therapeutic trial of donepezil in FTD failed to show any efficacy and a subgroup of patients experienced worsening of symptoms (Mendez et al., 2007).

Currently, cholinergic medication may be prescribed off-label in clinical practice for PPA patients who are amyloid positive (amyloid-PET or CSF amyloid/tau). AChE-PET allows one to directly discriminate PPA cases with a cholinergic deficit from those without a cholinergic deficit. This distinction could possibly predict a therapeutic response, but this remains to be demonstrated. The cholinergic deficit in LV in the current study provides a potential rationale for off-label use of AChE inhibitors (AChEI) in LV PPA due to underlying AD pathology. However our findings do not provide direct support for the use of AChEI in SV PPA, since AChE activity appears to be already naturally increased in this subtype compared to healthy controls.

4.4. Potential study limitations

The number of PPA patients included is small. This is inherent to the relatively high demands of the scanning procedures, in particular for dynamic PET acquisition with arterial sampling, and the relatively low prevalence of PPA (Gorno-Tempini et al., 2011). We calculated k_3 as index for AChE activity based on the well-established theoretical two-tissue three-rate constant compartment model with a cerebral blood volume fraction (Koeppe et al., 1999). Cerebral atrophy does not influence the rate constants including k_3, nor does k_3 depend on blood flow or aging (Kuhl et al., 1999). Based on the compartment model used, partial volume effects on k_3 are negligible if spillover from neighboring regions can be neglected (Koeppe et al., 1999; Kuhl et al., 1999). The effects of butyrylcholinesterase (BChE), which has been shown to increase in the course of neurodegenerative diseases (Nordberg et al., 2013), on the k_3 values are also negligible (Kuhl et al., 1999).

The diffuse structure of the BF itself may cause difficulties to reliably delineate its borders on MRI. We therefore used the BF mask obtained with a procedure of Kilimann (2014) based on histological staining of *post mortem* brain sections which were subsequently transferred to MNI space (Kilimann et al., 2014). Given the small volume of each subnucleus, we decided to assess the BF volume as one single volume as this provided a more robust estimation. The distribution of the current BF mask used in this study was compared to two previous masks, one based on a single subject (Teipel et al., 2005), and one probabilistic map based on 10 subjects (Zaborszky et al., 2008) in a study of Teipel and colleagues (Teipel et al., 2016). There was a high general agreement between all three masks. These findings suggest that the anatomy of the BF nuclei delineated by means of this procedure is relatively stable across subjects.

5. Conclusion

We established involvement of the cholinergic system in PPA, both at the structural and functional level. The observed cholinergic deficit further encourages development of cholinergic PPA treatments in LV, possibly in NFV but not in SV PPA cases.

Supplementary data to this article can be found online at http://dx.doi.org/10.1016/j.nicl.2016.11.027.

Acknowledgements

The authors report no disclosures relevant to the manuscript. Financial support was provided by the Inter-University Attraction Pole P6/29 (RV) and P7/11 (RV), KU Leuven OT/12/097 (RV, PD) and Programme Financing PFV 10/008 (RV, PD), Fund for Scientific Research - Flanders (FWO) G.0660.09N (RV, PD), Geneeskundige Stichting Koningin Elisabeth, Flanders Innovation & Entrepreneurship grant VIND. RV is a senior clinical investigator of the FWO.

The authors would like to thank the staff of Nuclear Medicine, Neurology and Radiology at the University Hospitals Leuven. Special thanks to PhD Grothe M. and MD, PhD Teipel S. for sharing their BF mask, Schildermans C., and Porters K. for assistance with the study. Also many thanks to the patients, their family and the volunteers who made this work possible.

References

Aggleton, J.P., Friedman, D.P., Mishkin, M., 1987. A comparison between the connections of the amygdala and hippocampus with the basal forebrain in the macaque. Exp. Brain Res. 67, 556–568.

Ashburner, J., Friston, K.J., 2000. Voxel-based morphometry–the methods. NeuroImage 11:805–821. http://dx.doi.org/10.1006/nimg.2000.0582.

Baker-Nigh, A., Vahedi, S., Davis, E.G., Weintraub, S., Bigio, E.H., Klein, W.L., Geula, C., 2015. Neuronal amyloid-β accumulation within cholinergic basal forebrain in ageing and Alzheimer's disease. Brain 138:1722–1737. http://dx.doi.org/10.1093/brain/awv024.

Berthier, M.L., Green, C., Higueras, C., Fernández, I., Hinojosa, J., Martín, M.C., 2006. A randomized, placebo-controlled study of donepezil in poststroke aphasia. Neurology 67: 1687–1689. http://dx.doi.org/10.1212/01.wnl.0000242626.69666.e2.

Boban, M., Kostovic, I., Simic, G., 2006. Nucleus subputaminalis: neglected part of the basal nucleus of Meynert [1]. Brain 129:2005–2006. http://dx.doi.org/10.1093/brain/aw1025.

Bohnen, N.I., Kaufer, D.I., Hendrickson, R., Ivanco, L.S., Lopresti, B., Davis, J.G., Constantine, G., Mathis, C.A., Moore, R.Y., DeKosky, S.T., 2005. Cognitive correlates of alterations in acetylcholinesterase in Alzheimer's disease. Neurosci. Lett. 380:127–132. http://dx.doi.org/10.1016/j.neulet.2005.01.031.

Bohnen, N.I., Kaufer, D.I., Ivanco, L.S., Lopresti, B., Koeppe, R.A., Davis, J.G., Mathis, C.A., Moore, R.Y., DeKosky, S.T., 2003. Cortical cholinergic function is more severely affected in parkinsonian dementia than in Alzheimer disease: an in vivo positron emission tomographic study. Arch. Neurol. 60:1745–1748. http://dx.doi.org/10.1001/archneur.60.12.1745.

Boxer, A.L., Knopman, D.S., Kaufer, D.I., Grossman, M., Onyike, C., Graf-Radford, N., Mendez, M., Kerwin, D., Lerner, A., Wu, C.-K., Koestler, M., Shapira, J., Sullivan, K., Klepac, K., Lipowski, K., Ullah, J., Fields, S., Kramer, J.H., Merrilees, J., Neuhaus, J., Mesulam, M.M., Miller, B.L., 2013. Memantine in patients with frontotemporal lobar degeneration: a multicentre, randomised, double-blind, placebo-controlled trial. Lancet Neurol. 12:149–156. http://dx.doi.org/10.1016/S1474-4422(12)70320-4.

Brambati, S.M., Renda, N.C., Rankin, K.P., Rosen, H.J., Seeley, W.W., Ashburner, J., Weiner, M.W., Miller, B.L., Gorno-Tempini, M.L., 2007. A tensor based morphometry study of longitudinal gray matter contraction in FTD. NeuroImage 35:998–1003. http://dx.doi.org/10.1016/j.neuroimage.2007.01.028.

Crawford, J.R., Garthwaite, P.H., 2012. Single-case research in neuropsychology: a comparison of five forms of t-test for comparing a case to controls. Cortex 48:1009–1016. http://dx.doi.org/10.1016/j.cortex.2011.06.021.

Dickson, D.W., 1999. Neuropathologic differentiation of progressive supranuclear palsy and corticobasal degeneration. J. Neurol. 246 (Suppl. II), 6–15.

Ferris, S.H., Farlow, M., 2013. Language impairment in Alzheimer's disease and benefits of acetylcholinesterase inhibitors. Clin. Interv. Aging 8:1007–1014. http://dx.doi.org/10.2147/CIA.S39959.

Gillebert, C.R., Schaeverbeke, J., Bastin, C., Neyens, V., Bruffaerts, R., De Weer, A.-S., Seghers, A., Sunaert, S., Van Laere, K., Versijpt, J., Vandenbulcke, M., Salmon, E., Todd, J.T., Orban, G.A., Vandenberghe, R., 2015. 3D shape perception in posterior cortical atrophy: a visual neuroscience perspective. J. Neurosci. 35:12673–12692. http://dx.doi.org/10.1523/JNEUROSCI.3651-14.2015.

Gorno-Tempini, M.L., Hillis, A.E., Weintraub, S., Kertesz, A., Mendez, M., Cappa, S.F., Ogar, J.M., Rohrer, J.D., Black, S., Boeve, B.F., Manes, F., Dronkers, N.F., Vandenberghe, R., Rascovsky, K., Patterson, K., Miller, B.L., Knopman, D.S., Hodges, J.R., Mesulam, M.M., Grossman, M., 2011. Classification of primary progressive aphasia and its variants. Neurology 76, 1–10.

Grossman, M., 2010. Primary progressive aphasia: clinicopathological correlations. Nat. Rev. Neurol. 6:88–97. http://dx.doi.org/10.1038/nrneurol.2009.216.
Grothe, M.J., Schuster, C., Bauer, F., Heinsen, H., Prudlo, J., Teipel, S.J., 2014. Atrophy of the cholinergic basal forebrain in dementia with Lewy bodies and Alzheimer's disease dementia. J. Neurol. 261:1939–1948. http://dx.doi.org/10.1007/s00415-014-7439-z.
Grube, M., Bruffaerts, R., Schaeverbeke, J., Neyens, V., De Weer, A.-S., Seghers, A., Bergmans, B., Dries, E., Griffiths, T.D., Vandenberghe, R., 2016. Core auditory processing deficits in primary progressive aphasia. Brain http://dx.doi.org/10.1093/brain/aww067.
Hirano, S., Shinotoh, H., Kobayashi, T., Tsuboi, Y., Wszolek, Z.K., Aotsuka, A., Tanaka, N., Ota, T., Fukushi, K., Tanada, S., Irie, T., 2006. Brain acetylcholinesterase activity in FTDP-17 studied by PET. Neurology 66:1276–1277. http://dx.doi.org/10.1212/01.wnl.0000208515.50924.94.
Hirano, S., Shinotoh, H., Shimada, H., Aotsuka, A., Tanaka, N., Ota, T., Sato, K., Ito, H., Kuwabara, S., Fukushi, K., Irie, T., Suhara, T., 2010. Cholinergic imaging in corticobasal syndrome, progressive supranuclear palsy and frontotemporal dementia. Brain 133: 2058–2068. http://dx.doi.org/10.1093/brain/awq120.
Hutsler, J.J., Gazzaniga, M.S., 1991. Acetylcholinesterase staining in human auditory and language cortices: regional variation of structural features. Cereb. Cortex 6, 260–270.
Irie, T., Fukushi, K., Namba, H., Iyo, M., Tamagami, H., Nagatsuka, S., Ikota, N., 1996. Brain acetylcholinesterase activity: validation of a PET tracer in a rat model of Alzheimer's disease. J. Nucl. Med. 37, 649–655.
Josephs, K.A., Stroh, A., Dugger, B., Dickson, D.W., 2009. Evaluation of subcortical pathology and clinical correlations in FTLD-U subtypes. Acta Neuropathol. 118:349–358. http://dx.doi.org/10.1007/s00401-009-0547-7.
Kasashima, S., Oda, Y., 2003. Cholinergic neuronal loss in the basal forebrain and mesopontine tegmentum of progressive supranuclear palsy and corticobasal degeneration. Acta Neuropathol. 105:117–124. http://dx.doi.org/10.1007/s00401-002-0621-x.
Kerbler, G.M., Fripp, J., Rowe, C.C., Villemagne, V.L., Salvado, O., Rose, S., Coulson, E.J., 2015. Basal forebrain atrophy correlates with amyloid β burden in Alzheimer's disease. NeuroImage. Clin. 7:105–113. http://dx.doi.org/10.1016/j.nicl.2014.11.015.
Kertesz, A., Morlog, D., Light, M., Blair, M., Davidson, W., Jesso, S., Brashear, R., 2008. Galantamine in frontotemporal dementia and primary progressive aphasia. Dement. Geriatr. Cogn. Disord. 25:178–185. http://dx.doi.org/10.1159/000113034.
Kilimann, I., Grothe, M., Heinsen, H., Alho, E.J.L., Grinberg, L., Amaro, E., Dos Santos, G.A.B., da Silva, R.E., Mitchell, A.J., Frisoni, G.B., Bokde, A.L.W., Fellgiebel, A., Filippi, M., Hampel, H., Klöppel, S., Teipel, S.J., 2014. Subregional basal forebrain atrophy in Alzheimer's disease: a multicenter study. J. Alzheimers Dis. 40:687–700. http://dx.doi.org/10.3233/JAD-132345.
Koeppe, R.A., Frey, K.A., Snyder, S.E., Meyer, P., Kilbourn, M.R., Kuhl, D.E., 1999. Kinetic modeling of N-[11C]methylpiperidin-4-yl propionate: alternatives for analysis of an irreversible positron emission tomography trace for measurement of acetylcholinesterase activity in human brain. J. Cereb. Blood Flow Metab. 19:1150–1163. http://dx.doi.org/10.1097/00004647-199910000-00012.
Kuhl, D.E., Koeppe, R.A., Minoshima, S., Snyder, S.E., Ficaro, E.P., Foster, N.L., Frey, K.A., Kilbourn, M.R., 1999. In vivo mapping of cerebral acetylcholinesterase activity in aging and Alzheimer's disease. Neurology 52:691–699. http://dx.doi.org/10.1212/WNL.52.4.691.
Matías-Guiu, J.A., Cabrera-Martín, M.N., Moreno-Ramos, T., Valles-Salgado, M., Fernandez-Matarrubia, M., Carreras, J.L., Matías-Guiu, J., 2015. Amyloid and FDG-PET study of logopenic primary progressive aphasia: evidence for the existence of two subtypes. J. Neurol. 262:1463–1472. http://dx.doi.org/10.1007/s00415-015-7738-z.
Mendez, M.F., Shapira, J.S., McMurtray, A., Licht, E., 2007. Preliminary findings: behavioral worsening on donepezil in patients with frontotemporal dementia. Am. J. Geriatr. Psychiatry 15:84–87. http://dx.doi.org/10.1097/01.JGP.0000231744.69631.33.
Mesulam, M.-M., 2013. Cholinergic circuitry of the human nucleus basalis and its fate in Alzheimer's disease. J. Comp. Neurol. 521:4124–4144. http://dx.doi.org/10.1002/cne.23415.
Mummery, C.J., Patterson, K., Price, C.J., Ashburner, J., Frackowiak, R.S., Hodges, J.R., 2000. A voxel-based morphometry study of semantic dementia: relationship between temporal lobe atrophy and semantic memory. Ann. Neurol. 47, 36–45.
Nordberg, A., Ballard, C., Bullock, R., Darreh-Shori, T., Somogyi, M., 2013. A review of butyrylcholinesterase as a therapeutic target in the treatment of Alzheimer's disease. Prim. Care Companion CNS Disord. 15. http://dx.doi.org/10.4088/PCC.12r01412.
Odawara, T., Shiozaki, K., Iseki, E., Hino, H., Kosaka, K., 2003. Alterations of muscarinic acetylcholine receptors in atypical Pick's disease without Pick bodies. J. Neurol. Neurosurg. Psychiatry 74, 965–967.
Poline, J.B., Worsley, K.J., Evans, A.C., Friston, K.J., 1997. Combining spatial extent and peak intensity to test for activations in functional imaging. NeuroImage 5:83–96. http://dx.doi.org/10.1006/nimg.1996.0248.
Procter, A.W., Qurne, M., Francis, P.T., 1999. Neurochemical features of frontotemporal dementia. Dement. Geriatr. Cogn. Disord. 10 (Suppl. 1), 80–84 (doi:51219).
Rosen, H.J., Gorno-Tempini, M.L., Goldman, W.P., Perry, R.J., Schuff, N., Weiner, M., Feiwell, R., Kramer, J.H., Miller, B.L., 2002. Patterns of brain atrophy in frontotemporal dementia and semantic dementia. Neurology 58:198–208. http://dx.doi.org/10.1212/WNL.58.2.198.
Schegg, K.M., Harrington, L.S., Neilsen, S., Zweig, R.M., Peacock, J.H., 1992. Soluble and membrane-bound forms of brain acetylcholinesterase in Alzheimer's disease. Neurobiol. Aging 13, 697–704.
Selden, N.R., Gitelman, D.R., Salamon-Murayama, N., Parrish, T.B., Mesulam, M.M., 1998. Trajectories of cholinergic pathways within the cerebral hemispheres of the human brain. Brain 121 (Pt 1), 2249–2257.
Shinotoh, H., 2007. Imaging of brain acetylcholinesterase activity in dementias and extrapyramidal disorders. Rinshō Shinkeigaku = Clin. Neureol. 47, 822–825.
Shinotoh, H., Namba, H., Yamaguchi, M., Fukushi, K., Nagatsuka, S., Iyo, M., Asahina, M., Hattori, T., Tanada, S., Irie, T., 1999. Positron emission tomographic measurement of acetylcholinesterase activity reveals differential loss of ascending cholinergic systems in Parkinson's disease and progressive supranuclear palsy. Ann. Neurol. 46, 62–69.
Silveyra, M.-X., García-Ayllón, M.-S., de Barreda, E.G., Small, D.H., Martínez, S., Avila, J., Sáez-Valero, J., 2012. Altered expression of brain acetylcholinesterase in FTDP-17 human tau transgenic mice. Neurobiol. Aging 33 (624):e23–e34. http://dx.doi.org/10.1016/j.neurobiolaging.2011.03.006.
Simić, G., Mrzljak, L., Fucić, A., Winblad, B., Lovrić, H., Kostović, I., 1999. Nucleus subputaminalis (Ayala): the still disregarded magnocellular component of the basal forebrain may be human specific and connected with the cortical speech area. Neuroscience 89, 73–89.
Snyder, S.E., Tluczek, L., Jewett, D.M., Nguyen, T.B., Kuhl, D.E., Kilbourn, M.R., 1998. Synthesis of 1-[11C]methylpiperidin-4-yl propionate ([11C]PMP) for in vivo measurements of acetylcholinesterase activity. Nucl. Med. Biol. 25:751–754. http://dx.doi.org/10.1016/S0969-8051(98)00045-6.
Tagliavini, F., Pilleri, G., Bouras, C., Constantinidis, J., 1984. The basal nucleus of Meynert in patients with progressive supranuclear palsy. Neurosci. Lett. 44, 37–42.
Tanaka, Y., Miyazaki, M., Albert, M.L., 1997. Effects of increased cholinergic activity on naming in aphasia. Lancet 350:116–117 (London, England). 10.1016/S0140-6736(05)61820-X.
Teipel, S., Raiser, T., Riedl, L., Riederer, I., Schroeter, M.L., Bisenius, S., Schneider, A., Kornhuber, J., Fliessbach, K., Spottke, A., Grothe, M.J., Prudlo, J., Kassubek, J., Ludolph, A., Landwehrmeyer, B., Straub, S., Otto, M., Danek, A., FTLDc Study Group, 2016. Atrophy and structural covariance of the cholinergic basal forebrain in primary progressive aphasia. Cortex 83:124–135. http://dx.doi.org/10.1016/j.cortex.2016.07.004.
Teipel, S.J., Flatz, W., Ackl, N., Grothe, M., Kilimann, I., Bokde, A.L.W., Grinberg, L., Amaro, E., Kljajevic, V., Alho, E., Knels, C., Ebert, A., Heinsen, H., Danek, A., 2014. Brain atrophy in primary progressive aphasia involves the cholinergic basal forebrain and Ayala's nucleus. Psychiatry Res. Neuroimaging 221:187–194. http://dx.doi.org/10.1016/j.pscychresns.2013.10.003.
Teipel, S.J., Flatz, W.H., Heinsen, H., Bokde, A.L.W., Schoenberg, S.O., Stöckel, S., Dietrich, O., Reiser, M.F., Möller, H.J., Hampel, H., 2005. Measurement of basal forebrain atrophy in Alzheimer's disease using MRI. Brain 128:2626–2644. http://dx.doi.org/10.1093/brain/awh589.
Tzourio-Mazoyer, N., Landeau, B., Papathanassiou, D., Crivello, F., Etard, O., Delcroix, N., Mazoyer, B., Joliot, M., 2002. Automated anatomical labeling of activations in SPM using a macroscopic anatomical parcellation of the MNI MRI single-subject brain. NeuroImage 15:273–289. http://dx.doi.org/10.1006/nimg.2001.0978.
Vandenberghe, R., 2016. Classification of the primary progressive aphasias: principles and review of progress since 2011. Alzheimers Res. Ther. 8:16. http://dx.doi.org/10.1186/s13195-016-0185-y.
Wallin, A., Sjögren, M., Blennow, K., Davidsson, P., 2003. Decreased cerebrospinal fluid acetylcholinesterase in patients with subcortical ischemic vascular dementia. Dement. Geriatr. Cogn. Disord. 16, 200–207 (doi:72803).
Wevers, A., 2011. Localisation of pre- and postsynaptic cholinergic markers in the human brain. Behav. Brain Res. 221:341–355. http://dx.doi.org/10.1016/j.bbr.2010.02.025.
Whitwell, J.L., Sampson, E.L., Watt, H.C., Harvey, R.J., Rossor, M.N., Fox, N.C., 2005. A volumetric magnetic resonance imaging study of the amygdala in frontotemporal lobar degeneration and Alzheimer's disease. Dement. Geriatr. Cogn. Disord. 20:238–244. http://dx.doi.org/10.1159/000087343.
Yoon, S.Y., Kim, J.-K., An, Y.-S., Kim, Y.W., 2015. Effect of donepezil on Wernicke Aphasia after bilateral middle cerebral artery infarction: subtraction analysis of brain F-18 fluorodeoxyglucose positron emission tomographic images. Clin. Neuropharmacol. 38:147–150. http://dx.doi.org/10.1097/WNF.0000000000000089.
Zaborszky, L., Csordas, A., Mosca, K., Kim, J., Gielow, M.R., Vadasz, C., Nadasdy, Z., 2015. Neurons in the basal forebrain project to the cortex in a complex topographic organization that reflects corticocortical connectivity patterns: an experimental study based on retrograde tracing and 3D reconstruction. Cereb. Cortex 25:118–137. http://dx.doi.org/10.1093/cercor/bht210.
Zaborszky, L., Hoemke, L., Mohlberg, H., Schleicher, A., Amunts, K., Zilles, K., 2008. Stereotaxic probabilistic maps of the magnocellular cell groups in human basal forebrain. NeuroImage 42:1127–1141. http://dx.doi.org/10.1016/j.neuroimage.2008.05.055.